

Optical Constants of HNO₃/H₂O and H₂SO₄/HNO₃/H₂O at Low Temperatures in the Infrared Region

C. E. Lund Myhre,[†] H. Grothe,[‡] A. A. Gola,^{†,§} and C. J. Nielsen^{*,†}

Department of Chemistry, University of Oslo, P.O. Box 1033, Blindern, N-0372 Oslo, Norway, and Institute of Materials Chemistry, Vienna University of Technology, Veterinärplatz 1, A-1210 Vienna, Austria

Received: February 17, 2005; In Final Form: June 20, 2005

The complex index of refraction of liquid HNO₃/H₂O and H₂SO₄/HNO₃/H₂O has been obtained at different temperatures and acid concentrations. FT-IR specular reflectance spectra were obtained for 30, 54, and 64 wt % aqueous HNO₃ and for four different H₂SO₄/HNO₃/H₂O mixtures in the temperature region from 293 to 183 K. The complex index of refraction was obtained from the reflectance spectra with the Kramers–Kronig transformation. The optical constants of the binary and ternary mixtures vary with the acid concentration and the temperature. The results demonstrate that vibrational bands originating from the sulfate species are more sensitive to changes in temperature than the bands originating from vibrations in the nitrate species; only minor changes in the nitrate vibrational bands are observed as the temperature decreases below 248 K.

1. Introduction

It is well established that polar stratospheric clouds (PSCs) are linked to ozone depletion and the development of the so-called “ozone hole”.^{1,2} PSCs mainly consist of liquid or solid nitric acid, sulfuric acid, and water and are commonly classified in subgroups on the basis of their composition and phase as described by, for example, Seinfeld and Pandis,³ Zondlo and co-workers,⁴ and Tolbert and Toon.⁵ Type Ib PSCs are spherical liquid ternary solution droplets of sulfuric acid, nitric acid, and water: H₂SO₄/HNO₃/H₂O (SNW). It is assumed that they are formed from stratospheric sulfuric acid aerosols which take up increasing amounts of H₂O and HNO₃ from the gas phase as response to a decrease in temperature.^{4,6} As the temperature drops, additional H₂O and HNO₃ condense onto the aerosol, thus sulfuric acid constitutes only a minor mole fraction at temperatures below 190 K.^{6,7}

Satellite and sonde measurements employing optical scattering techniques have commonly been used in observations of stratospheric aerosols.^{8–13} Mid-infrared remote-sensing instruments are used to derive the chemical composition, aerosol phase, and size distribution of stratospheric as well as tropospheric aerosols. The interpretation of the measured spectra requires laborious retrieval algorithms commonly involving Mie theory in which the complex index of refraction is an essential parameter.^{11–18} The complex index of refraction is defined by $\tilde{N}(\tilde{\nu}) = n(\tilde{\nu}) + ik(\tilde{\nu})$; $n(\tilde{\nu})$ and $k(\tilde{\nu})$ are the wavenumber dependent refractive and absorption indices or optical constants, respectively. Together, they accurately define the full optical behavior of the material under investigation.

Several data sets of the complex index of refraction in the infrared region at temperatures relevant to the stratosphere exist for both the H₂SO₄/H₂O and HNO₃/H₂O systems.^{19–27} However, significant discrepancies exist between them. Wagner et al.²⁸

reported a quantitative test of the available optical constants of H₂SO₄/H₂O and HNO₃/H₂O mixtures relevant to the stratospheric aerosols. They designed an experiment in the large aerosol chamber AIDA in Karlsruhe, Germany, in which they recorded extinction spectra of supercooled aerosols of H₂SO₄/H₂O at three different conditions and HNO₃/H₂O at two different conditions. They tested the different optical constant data sets by comparing measured aerosol data with those retrieved from the analysis of the extinction spectra. For H₂SO₄/H₂O, they found very good agreement using the data of Niedziela et al.²¹ for all the three experimental conditions. The data presented by Lund Myhre et al.²⁰ only cover one of the conditions they examined; the agreement, however, was excellent. The largest differences with the experiment were observed using the optical constants reported by Biermann et al.,¹⁹ which also deviate substantially from those of Lund Myhre et al.²⁰ and Niedziela et al.²¹ For HNO₃/H₂O, the results of the aerosol experiments were in fair agreement with the data of Norman et al.,²³ but not as good as that for the H₂SO₄/H₂O system. Also the HNO₃/H₂O optical constants of Biermann et al.¹⁹ were in lesser agreement with the chamber experiments.

Only two studies report optical constants in the infrared region for the ternary H₂SO₄/HNO₃/H₂O system.^{19,29} In addition to optical constants, Biermann et al.¹⁹ also presented a linear mixing scheme to predict the optical constants of ternary mixtures from the binary data sets of H₂SO₄/H₂O and HNO₃/H₂O, and they compared their model results with experimental optical constants of 5 ternary mixtures at different temperatures. Unfortunately, their experimental optical constants for the ternary mixtures were only presented in graphical form. Norman et al.²⁹ reported optical constants of six different ternary mixtures at 220 K: the mixtures had ~45 wt % H₂O and varying amounts of H₂SO₄ and HNO₃. There are significant discrepancies between the experimental data of Norman et al.²⁹ and the predictions from the model by Biermann et al.¹⁹ In summary, there is still a lack of data for the HNO₃/H₂O system and particularly for the H₂SO₄/HNO₃/H₂O system.

The present study addresses the optical constants of the binary HNO₃/H₂O and the ternary H₂SO₄/HNO₃/H₂O systems. We

* E-mail: c.j.nielsen@kjemi.uio.no.

[†] University of Oslo.

[‡] Vienna University of Technology.

[§] Permanent address: Department of Physical Chemistry, Medical University of Wrocław, Pl. Nankiera, 50-140 Wrocław, Poland.

TABLE 1. List of Measured HNO₃/H₂O and H₂SO₄/HNO₃/H₂O Spectra

H ₂ SO ₄ /HNO ₃ /H ₂ O		temp (K)
wt %	mol %	
0/30/70	0/11/89	223, 233, 243, 253, 273, 293
0/54/46	0/25/75	243, 248, 253, 273, 293
0/64/36	0/34/66	238, 243, 253, 273, 293
4/46/50	1/21/78	223, 253, 273, 293
21/23/56	6/10/84	203, 213, 223, 253, 273, 293
25/17/58	7/7/86	183, 193, 203, 213, 223, 253, 273, 293
28/14/58	8/6/86	183, 193, 203, 213, 223, 253, 273, 293

present the absorption index, $k(\tilde{\nu})$, and the refractive index, $n(\tilde{\nu})$, in the region from 6500 to 400 cm⁻¹. Table 1 summarizes the temperatures at which the binary and ternary mixtures were investigated. The optical constants are available as Supporting Information.

2. Experimental Section

2.1. Reflectance Measurements. The experimental method and calculation procedure applied in the infrared region has previously been described in detail²⁰ and only the main principles are reported here. Specular reflectance spectra at near normal incident were obtained with a Perkin-Elmer System 2000 FTIR spectrometer in the region of 6700–400 cm⁻¹. The spectrometer is equipped with a room-temperature DTGS detector and the spectra were obtained at a nominal resolution of 4 cm⁻¹ by averaging 64 scans. Far-infrared spectra (700–20 cm⁻¹) were obtained with a Bruker IFS HR120 instrument equipped with DTGS and He-cooled bolometer detectors. A simple modification of the optical beam path in a standard specular reflection unit allows the surface of the sample support to be oriented horizontally which makes liquid surface studies feasible. The equipment was designed for infinitely thick samples to avoid reflections from the back of the sample: in this case, 14 mm was more than adequate. The sample holder (volume 13.5 cm³ and surface area of 9.5 cm²) was temperature regulated by a stream of cold nitrogen. The temperature was controlled to within ±0.5 K, measured inside the samples during the recording of the spectra. The entire optical setup was enclosed in a 1 L environmental chamber, which was purged with around 10 mL of N₂/min (99.996% N₂, H₂O < 5 ppm, AGA) to keep the relative humidity constant and low and thereby prevent water vapor from condensing on the sample. Far-IR reflectance spectra were recorded at room temperature.

The experimental specular reflectance spectra, $R(\tilde{\nu})$, were obtained as a ratio of two single-beam spectra, $I(\tilde{\nu})$ and $I_0(\tilde{\nu})$, where $I(\tilde{\nu})$ is the intensity of the radiant flux reflected from the sample surface and $I_0(\tilde{\nu})$ is the intensity of the radiant flux reflected from a gold plated mirror which exhibits constant reflectivity close to unity over the IR region under investigation. The complex index of refraction was derived by the use of the Kramers–Kronig analysis of the specular reflectance spectra, $R(\nu)$, spanning the 6500–60 cm⁻¹ region and obtained at near normal incidence. In the case of perpendicular incidence of light, the boundary conditions give Fresnel's relationship

$$R(\nu) = \left| \frac{\tilde{N}(\nu) - 1}{\tilde{N}(\nu) + 1} \right|^2 \quad (1)$$

$\tilde{N}(\nu)$ is the complex index of refraction. The change of phase between the incident and reflected beam, $\phi(\nu)$, may be obtained by employing the Kramers–Kronig transformation

$$\phi(\nu_m) = \frac{2\nu_m}{\pi} \int_0^\infty \frac{\ln(\sqrt{R(\nu)})}{\nu^2 - \nu_m^2} d\nu \quad (2)$$

in which the integral is a Cauchy principal value integral and which enables one to calculate both $n(\nu)$ and $k(\nu)$ from $R(\nu)$

$$n(\nu) = \frac{1 - R(\nu)}{1 + R(\nu) - 2\sqrt{R(\nu)} \cos(\phi(\nu))} \quad (3)$$

$$k(\nu) = \frac{-2\sqrt{R(\nu)} \sin(\phi(\nu))}{1 + R(\nu) - 2\sqrt{R(\nu)} \cos(\phi(\nu))} \quad (4)$$

The algorithm used in the present work is integrated in the Perkin-Elmer FT-IR spectrometer software.³⁰ The computations are based on the following assumptions: (i) the samples must be homogeneous, (ii) the specular reflectance beam must be measured at an angle of less than 10° from the perpendicular, and (iii) the sample must be thick enough to ensure that no light is reflected from the backside to prevent internal reflection effects. When studying aqueous solutions, these assumptions are easily fulfilled for the infrared spectral region. The algorithm also assumes that the spectral cutoff falls in a moderately flat unstructured region. This requirement comes from the evaluation of the integral (eq 2) and the implicit requirement of $R(\nu_\infty)$. In the low-wavenumber region, the condition of spectral flatness is not strictly fulfilled and neglecting this condition can lead to large errors in the derived refractive and absorption indices.²⁰ To avoid this type of error, it is necessary to include the specular reflectance spectrum of the far-infrared region prior to the Kramers–Kronig transformation. The main advantage of using the Kramers–Kronig transformation from reflectivity, $R(\nu)$, to the phase-shift, $\phi(\nu)$, compared to using absorption data, is that it does not require exact knowledge about the optical path length in the absorbing medium. Least-squares refinement calculations are also avoided.

On the basis of our previous examination of water as well as aqueous H₂SO₄ reflectance spectra,²⁰ we estimate the relative uncertainty in our results to be within 2% for the refractive indices and 3% for the absorption indices: the uncertainties are mainly determined by the accuracy of the experimental specular reflectance spectra.

2.2. Raman Spectra. Raman spectra were obtained with a DILOR RTI30 spectrometer using the 514.5 nm line of an argon ion laser (Spectra Physics model 2000) with 90° excitation. The nominal resolution was around 3.5 cm⁻¹ in all spectra. The samples were studied in capillary tubes of ca. 2 mm inner diameter surrounded by a Dewar and cooled by gaseous nitrogen evaporated from a reservoir.³¹ Molal Raman scattering intensities of selected HNO₃ and NO₃⁻ bands were obtained with a HORIBA LabRam instrument.

2.3. Sample Preparation. The binary mixtures of HNO₃/H₂O were prepared from a 70 wt % HNO₃/H₂O solution of p.a. quality (Fluka) and distilled water. The ternary mixtures were prepared from the same 70 wt % solution of HNO₃/H₂O, concentrated H₂SO₄ of p.a. quality (96–98% in H₂O, Fluka), and distilled water. The concentrations in the individual binary and ternary solutions, determined by titration, are accurate within 0.2%. Figure 1 is a ternary diagram showing the compositions of the samples studied. The ternary mixtures were selected to match aerosol chamber experiments in which the uptake of water and nitric acid on a given sulfuric acid aerosol had been monitored.³²

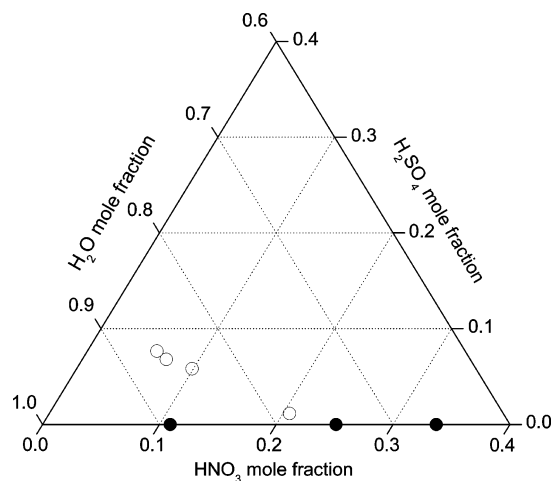


Figure 1. Composition of the binary $\text{HNO}_3/\text{H}_2\text{O}$ (●) and ternary $\text{H}_2\text{SO}_4/\text{HNO}_3/\text{H}_2\text{O}$ (○) mixtures studied.

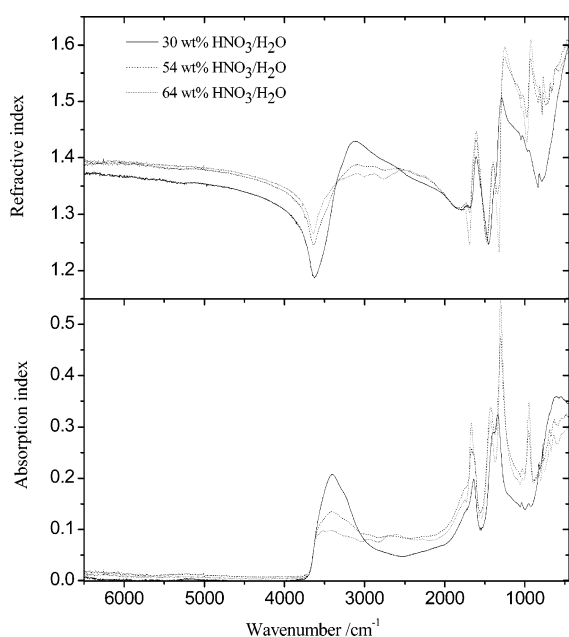


Figure 2. Refractive and absorption index at room temperature of binary mixtures of 30, 54, and 64 wt % $\text{HNO}_3/\text{H}_2\text{O}$.

3. Results and Discussion

3.1. Optical Constants of $\text{HNO}_3/\text{H}_2\text{O}$. Figure 2 illustrates the variation in the refractive and absorption indices of the binary $\text{HNO}_3/\text{H}_2\text{O}$ system at 293 K as a function of acid concentration. The absorption and refractive index spectra change considerably with the weight percent of the acid because of the different concentrations of the constituents HNO_3 , NO_3^- , and H_3O^+ . Figure 3 illustrates the variation in the absorption indices with temperature of 30 ($x_{\text{HNO}_3} = 0.11$) and 54 wt % ($x_{\text{HNO}_3} = 0.25$) aqueous HNO_3 . There are some distinct differences between the absorption indices of the two mixtures. For the 30 wt % solution, the spectra show that the intensities of the bands are changing with temperature down to approximately 253 K. At lower temperatures, only very small changes are observed in the spectra. For the 54 wt % solution, the variations in the spectra with temperature are even smaller: only minor changes in the spectra are observed as the temperature drops below 273 K. The results for the 64 wt % ($x_{\text{HNO}_3} = 0.34$) solution are in line with these observations. The observed trend in the optical constants with temperature is in general agreement with the results of Biermann et al.,¹⁹ who reported optical constants of

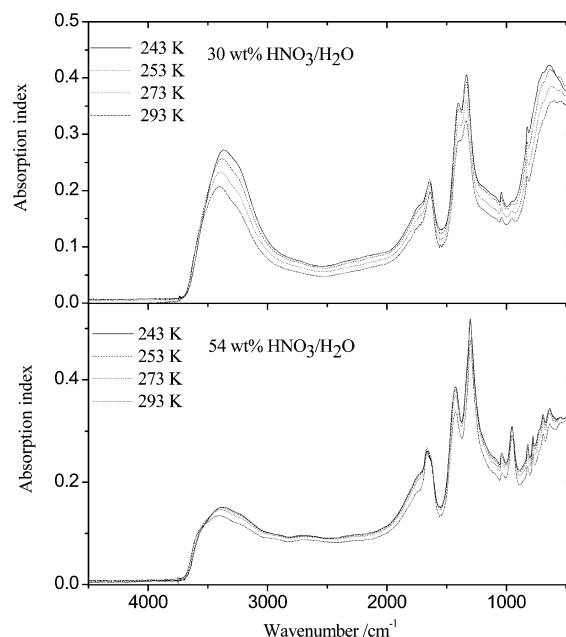


Figure 3. Variation in the absorption index of 30 and 54 wt % $\text{HNO}_3/\text{H}_2\text{O}$ mixtures caused by the change in the temperature.

the $\text{HNO}_3/\text{H}_2\text{O}$ system at temperatures from 293 to ca. 213 K and concentrations ranging from 10 to 54 wt %. The compositions and temperatures of our mixtures, however, do not exactly correspond to those investigated by Biermann et al.,¹⁹ and a direct comparison of results is not possible.

In Figure 4, we compare our optical constants for 54 and 64 wt % aqueous HNO_3 at 243 K with those obtained for supercooled aerosols at 220 K by Norman et al.²³ There are some discrepancies which probably have at least three origins. (1) There is a temperature difference between our samples and their samples which may explain some of the deviation, although the present results suggest this to be of minor importance. (2) There is a difference in the low-wavenumber cutoff in the Kramers–Kronig transformation which results in different truncation errors in the two studies. Norman et al.²³ have spliced their low-temperature iteratively refined $k(\tilde{\nu})$ ending at 750 cm^{-1} with a room-temperature $k(\tilde{\nu})$ from 780 to 400 cm^{-1} from the study by Query and Tyler,³³ while we have spliced our low-temperature reflectance spectra ending at 400 cm^{-1} with room-temperature reflectance spectra from 400 to 60 cm^{-1} . (3) The subtractive Kramers–Kronig transformation used by Norman et al.²³ requires an anchor point for $n(\tilde{\nu})$ at some wavenumber, and they used interpolated values from the Query and Tyler room-temperature data set,³³ corrected for changes in the density associated with cooling to 220 K. An error in the anchor points used will primarily show up as an offset on their final $n(\tilde{\nu})$ data, as is apparent in Figure 4. We note that our refractive indices in the near-infrared region are in agreement with the results of extrapolation model of Krieger et al.³⁴

3.2. Optical Constants of the $\text{H}_2\text{SO}_4/\text{HNO}_3/\text{H}_2\text{O}$ System.

The spectra of the ternary mixtures are more complex. Figure 5 illustrates the variation in the refractive and absorption indices at 223 K in the 6500 – 400 cm^{-1} range with composition. Figure 6 shows the absorption index of the ternary mixture 21 wt % H_2SO_4 , 23 wt % HNO_3 , 56 wt % H_2O (21/23/56 SNW) with the molecular origin of the bands indicated. The spectral variation with temperature is illustrated in Figure 7 which shows the absorption index of a 28/14/58 SNW mixture at temperatures ranging from 293 to 183 K. In these spectra, the bands originating from the vibrations in the sulfate species are clearly

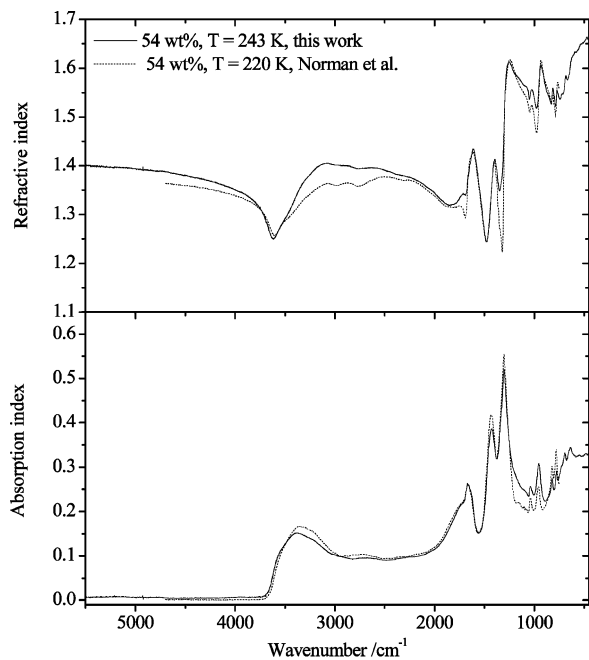


Figure 4. Comparison of our optical constant data with that of Norman et al.²³ Top: 54 wt % HNO₃/H₂O. Bottom: 64 wt % HNO₃/H₂O.

more sensitive to temperature change than the bands originating from the nitrate ion.

3.3. Ionic Speciation in the HNO₃/H₂O and H₂SO₄/HNO₃/H₂O Mixtures. Nitric and sulfuric acids are both strong acids in the aqueous phase, and the binary and ternary aqueous solutions are mixtures of different ionic constituents, as well as undissociated HNO₃ and H₂SO₄ in the most concentrated solutions. For the binary system H₂SO₄/H₂O, the dissociation of H₂SO₄ to bisulfate is known to be very close to one for concentrations below approximately 80 wt %. The dissociation of bisulfate, HSO₄⁻, was recently studied in the temperature range from 298 K down to stratospheric temperatures by Raman spectroscopy.²⁰ The results are in agreement with a new thermodynamic model presented by Knopf et al.³⁵

The degree of dissociation of aqueous HNO₃ has been addressed repeatedly by Raman spectroscopy. The first Raman

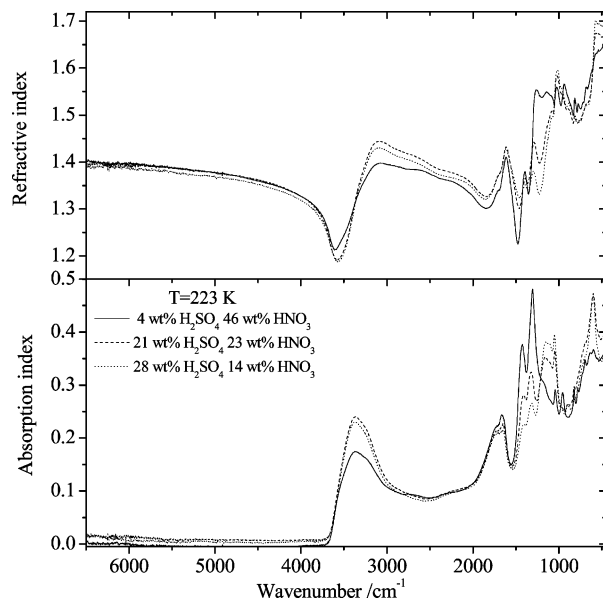


Figure 5. Refractive and absorption index at 223 K for the three ternary H₂SO₄/HNO₃/H₂O mixtures studied.

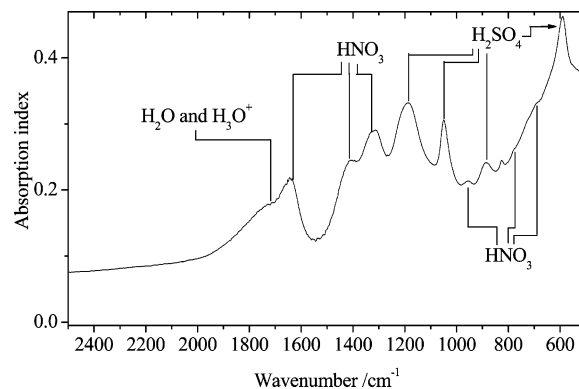


Figure 6. Absorption index of the ternary mixture of 21 wt % H₂SO₄, 23 wt % HNO₃, 56 wt % H₂O at room temperature with the origin of the bands included.

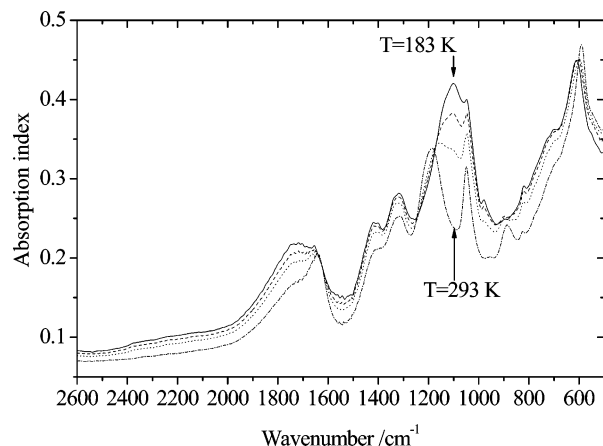


Figure 7. Absorption index of the ternary mixture of 25 wt % H₂SO₄, 17 wt % HNO₃, 58 wt % H₂O at the temperatures 293, 223, 203, and 183 K.

study of nitric acid was published 70 years ago,³⁶ and a complete spectral assignment appeared 10 years later.³⁷ A concurrent Raman study by Redlich and Giegelsen included a determination of the thermodynamic dissociation constant at room temperature,³⁸ and later Krawetz reported the variation in dissociation with acid concentration at 0, 25, and 50 °C.³⁹

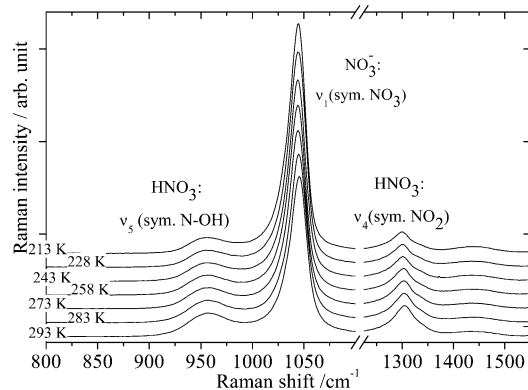


Figure 8. Raman spectra of 54 wt % $\text{HNO}_3/\text{H}_2\text{O}$ at seven different temperatures. The assignments of the bands are taken from Minogue et al.⁴⁰

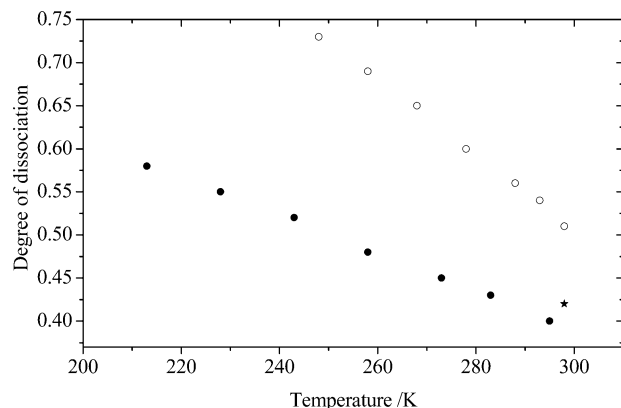


Figure 9. Degree of dissociation of 54 wt % $\text{HNO}_3/\text{H}_2\text{O}$ at seven different temperatures (●) compared with the data of Minogue et al.⁴⁰ (○) and the data of Krawetz³⁹ (★).

Recently, Minogue et al.⁴⁰ studied the dissociation in 54 ($x_{\text{HNO}_3} = 0.25$), 26 ($x_{\text{HNO}_3} = 0.09$), and 15 wt % ($x_{\text{HNO}_3} = 0.05$) HNO_3 solutions in the temperature range between 300 and 248 K by Raman spectroscopy. They reported a linear relationship between the degree of dissociation and temperature in the 248–300 K region. This is apparently in contrast to the observed leveling in our optical constants at lower temperatures. We therefore decided to replicate the Raman temperature study of the 54 wt % HNO_3 . The spectra are given in Figure 8, while Figure 9 shows the derived degrees of dissociation based on scattering coefficients measured relative to that of the $\nu_1(a_1)$ band of ClO_4^- , as previously described in our study of HSO_4^- dissociation.²⁰ The scattering coefficient of the $\nu_1(a_1)$ mode around 1047 cm^{-1} in NO_3^- was determined, relative to the $\nu_1(a_1)$ mode in ClO_4^- , to be 0.65 ± 0.01 , while the scattering intensity of the HNO_3 band around 955 cm^{-1} was determined to be 0.13 ± 0.01 . Figure 9 also includes the results of Minogue et al.⁴⁰ and Krawetz.³⁹ While our Raman study shows the same trend in the degree of dissociation with temperature as that of Minogue et al.,⁴⁰ our results are much lower and in better agreement with the early study of Krawetz.³⁹ One explanation of this discrepancy may be the fact that the symmetric NO_3 stretch in HNO_3 lies as a shoulder on the more intense NO_3^- band. Minogue et al.⁴⁰ recorded their Raman spectra with a resolution of 16 cm^{-1} , which shows the two bands as one. Careful band deconvolution of spectra with high resolution is essential to retrieve the degree of dissociation. Our spectral analysis showed that the line shapes of the Raman spectra changed when the temperature decreased indicating a modification of the molecular interactions in the solution at low

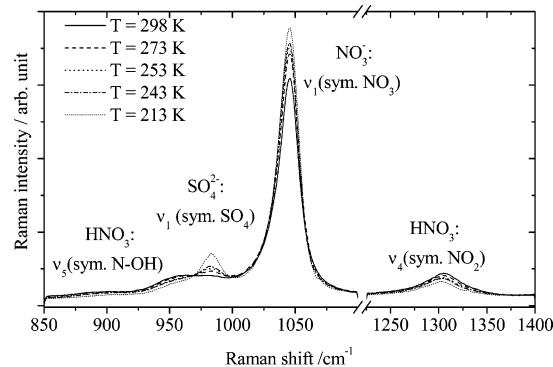


Figure 10. Raman spectra of 14 wt % H_2SO_4 , 46 wt % HNO_3 , 40 wt % H_2O at five different temperatures.

temperatures. Together with changes in density⁴¹ and equilibria, this tentatively explains the observed variation in the optical constants. The dominating bands in the IR spectrum of aqueous HNO_3 are found around 1420 cm^{-1} (NO_3^-) and 1310 cm^{-1} (HNO_3), the HNO_3 band being the stronger. As the temperature decreases, the density increases and the total number of molecules and ions per volume unit increases. Simultaneously, more HNO_3 dissociates. Thus, the change in the absorbance index of the H_2O bands essentially reflects the change in density as a function of temperature, while the absolute, as well as relative, change in the absorbance index of the $\text{HNO}_3/\text{NO}_3^-$ band pair reflects the increase in both the density and degree of dissociation.

For the optical constants of the ternary mixture, Figure 7 shows that the bands originating from bisulfate and sulfate change more than the bands originating from NO_3^- and HNO_3 . We have recorded the Raman spectrum of 14/46/40 wt % (0.2:1:3 mol ratio) $\text{H}_2\text{SO}_4/\text{HNO}_3/\text{H}_2\text{O}$ at 5 different temperatures, shown in Figure 10. The bands originating from vibrations in SO_4^- , as well as those in NO_3^- , are increasing continuously in the whole temperature range. However, a minor increase in the bands originating from vibrations in NO_3^- , as well as smaller decrease in the HNO_3 bands, is detected, compared with the binary mixture as the temperature is changing. This indicates that the dissociation equilibria of HNO_3 and H_2SO_4 interfere, which is in agreement with the results of Minogue,⁴⁰ who also investigated the spectral changes in ternary mixtures of $\text{H}_2\text{SO}_4/\text{HNO}_3/\text{H}_2\text{O}$ at different mixing ratios and temperatures semi-quantitatively by Raman spectroscopy. Their conclusion was that the complete ionization of the nitric acid subsystem occurs before the complete ionization of HSO_4^- , regardless of the concentration ratios employed. They explained this by the stronger acidity of nitric acid with respect to bisulfate.

So far, only the mixing scheme developed by Biermann et al.¹⁹ permits the calculation of optical constants of the ternary system covering a broad range of compositions and temperatures. However, as discussed by Wagner et al.,²⁸ the results from a Mie scattering calculation using the mixing scheme of Biermann et al.¹⁹ differ significantly from the experimental spectra. This is also reported by Norman et al.²⁹ and agrees with our observations when we employ their model and use our binary data sets. Rather than the quality of the binary data used in the parametrization, we agree with the suggestion of Norman et al.²⁹ that the reason for the deviations are mainly the result of the simplified mixing rule. Their model assumes no interaction between the two equilibria present in the system which is clearly not the case. The deviations are a consequence of molecular interactions between the ionic species present in the ternary mixtures modifying the bisulfate dissociation, as reported by Minogue et al.⁴⁰ and illustrated in Figure 10.

Summary and Conclusion

This study presents optical constants in the infrared spectral region of three binary HNO₃/H₂O and four ternary H₂SO₄/HNO₃/H₂O mixtures at a wide range of temperatures. The main absorption and refraction features of the systems are determined from the ionic speciation in the mixtures. The optical constants of the binary HNO₃/H₂O system varies very little in response to temperature changes below approximately 243 K for the three mixtures investigated, also reported by Biermann et al.¹⁹ In the ternary mixtures, the absorption bands for the sulfate species are much more sensitive to temperature change than the bands originating from vibrations in the nitrate ion and HNO₃. There are also indications that the degree of dissociation of HSO₄⁻ in the ternary mixtures is altered because of the presence of HNO₃. This is of importance for modeling and parametrization of multicomponent mixtures in the stratosphere and might be of atmospheric relevance in the remote sensing of stratospheric aerosols and the interpretation of the spectra. A more reliable model of the optical constants of ternary H₂SO₄/HNO₃/H₂O solutions requires a thorough understanding of ionic speciation in the system.

Acknowledgment. The present work was funded by the Research Council of Norway (Grant No. 123289/410). A.A.G. acknowledges a Government Scholarship under the cultural agreement between Norway and Poland. H.G. acknowledges a stipend from the University of Oslo, Program for International Cooperation, and financial support by the Vienna University of Technology. We thank Dr. Robert Wagner, Institute of Meteorology and Climate Research, Research Centre Karlsruhe, Germany for useful and helpful discussions.

Supporting Information Available: Optical constants for HNO₃/H₂O and H₂SO₄/HNO₃/H₂O in the 6500–450 cm⁻¹ region and Figures 2, 3, 5, 7, 8, and 10 in color. This material is available free of charge via the Internet at <http://pubs.acs.org>.

References and Notes

- (1) Solomon, S. *Nature* **1990**, *347*, 347.
- (2) Albritton, D. L.; Watson, R. T.; Solomon, S.; Hampson, R. F.; Ormond, F. *Scientific Assessment of Ozone Depletion: 1991*; World Meteorological Organization: Geneva, Switzerland, 1991.
- (3) Seinfeld, J. H.; Pandis, S. N. *Atmospheric Chemistry and Physics: From Air Pollution to Climate Change*; Wiley: New York, 1998.
- (4) Zondlo, M. A.; Hudson, P. K.; Prenni, A. J.; Tolbert, M. A. *Annu. Rev. Phys. Chem.* **2000**, *51*, 473.
- (5) Tolbert, M. A.; Toon, O. B. *Science* **2001**, *292*, 61.
- (6) Carslaw, K. S.; Luo, B. P.; Clegg, S. L.; Peter, T.; Brimblecombe, P.; Crutzen, P. J. *Geophys. Res. Lett.* **1994**, *21*, 2479.
- (7) Tabazadeh, A.; Jensen, E. J.; Toon, B.; Drdla, K.; Schoebert, M. R. *Science* **2001**, *291*, 2591.

- (8) Rosen, J. M.; Kjome, N. T.; Oltmans, S. J. *Geophys. Res. Lett.* **1990**, *17*, 1271.
- (9) Deshler, T.; Adriani, A.; Hofmann, D. J.; Gobbi, G. P. *Geophys. Res. Lett.* **1991**, *18*, 1999.
- (10) Baumgardner, D.; Dye, J. E.; Gandrud, B. W.; Knollenberg, R. G. *J. Geophys. Res., [Atmos.]* **1992**, *97*, 8035.
- (11) Massie, S. T.; Deshler, T.; Thomas, G. E.; Mergenthaler, J. L.; Russell, J. M. *J. Geophys. Res., [Atmos.]* **1996**, *101*, 23007.
- (12) Hayasaka, T.; Meguro, Y.; Sasano, Y.; Takamura, T. *Appl. Opt.* **1998**, *37*, 961.
- (13) Hervig, M. E.; Deshler, T.; Russell, J. M., III. *J. Geophys. Res., [Atmos.]* **1998**, *103*, 1573.
- (14) Russell, P. B.; Hobbs, P. V.; Stowe, L. L. *J. Geophys. Res., [Atmos.]* **1999**, *104*, 2213.
- (15) Redemann, J.; Turco, R. P.; Liou, K. N.; Russell, P. B.; Bergstrom, R. W.; Schmid, B.; Livingston, J. M.; Hobbs, P. V.; Hartley, W. S.; Ismail, S.; Ferrare, R. A.; Browell, E. V. *J. Geophys. Res., [Atmos.]* **2000**, *105*, 9949.
- (16) Nakajima, T.; Higurashi, A. *Geophys. Res. Lett.* **1998**, *25*, 3815.
- (17) Kaufman, Y. J.; Tanre, D.; Remer, L. A.; Vermote, E. F.; Chu, A.; Holben, B. N. *J. Geophys. Res., [Atmos.]* **1997**, *102*, 17051.
- (18) King, M. D.; Kaufman, Y. J.; Tanre, D.; Nakajima, T. *Bull. Am. Meteorol. Soc.* **1999**, *80*, 2229.
- (19) Biermann, U. M.; Luo, B. P.; Peter, T. *J. Phys. Chem. A* **2000**, *104*, 783.
- (20) Lund Myhre, C. E.; Christensen, D. H.; Nicolaisen, F. M.; Nielsen, C. J. *J. Phys. Chem. A* **2003**, *107*, 1979.
- (21) Niedziela, R. F.; Norman, M. L.; DeForest, C. L.; Miller, R. E.; Worsnop, D. R. *J. Phys. Chem. A* **1999**, *103*, 8030.
- (22) Niedziela, R. F.; Norman, M. L.; Miller, R. E.; Worsnop, D. R. *Geophys. Res. Lett.* **1998**, *25*, 4477.
- (23) Norman, M. L.; Qian, J.; Miller, R. E.; Worsnop, D. R. *J. Geophys. Res., [Atmos.]* **1999**, *104*, 30571.
- (24) Palmer, K. F.; Williams, D. *Appl. Opt.* **1975**, *14*, 208.
- (25) Pinkley, L. W.; Williams, D. *J. Opt. Soc. Am.* **1976**, *66*, 122.
- (26) Remsburg, E. E.; Lavery, D.; Crawford, B., Jr. *J. Chem. Eng. Data* **1974**, *19*, 263.
- (27) Tisdale, R. T.; Glandorf, D. L.; Tolbert, M. A.; Toon, O. B. *J. Geophys. Res., [Atmos.]* **1998**, *103*, 25353.
- (28) Wagner, R.; Mangold, A.; Moehler, O.; Saathoff, H.; Schnaiter, M.; Schurath, U. *Atmos. Chem. Phys.* **2003**, *3*, 1147.
- (29) Norman, M. L.; Miller, R. E.; Worsnop, D. R. *J. Phys. Chem. A* **2002**, *106*, 6075.
- (30) *Spectrum*, version 2.00; Perkin-Elmer: Boston, 1998.
- (31) Miller, F. A.; Harney, B. A. *Appl. Spectrosc.* **1970**, *24*, 291.
- (32) Wagner, R. Private communication.
- (33) Querry, M. R.; Tyler, I. L. *J. Chem. Phys.* **1980**, *72*, 2495.
- (34) Krieger, U. K.; Mossinger, J. C.; Luo, B.; Weers, U.; Peter, T. *Appl. Opt.* **2000**, *39*, 3691.
- (35) Knopf, D. A.; Luo, B. P.; Krieger, U. K.; Koop, T. *J. Phys. Chem. A* **2003**, *107*, 4322.
- (36) Anderhold, H.; Weiss, H. E. *Z. Phys.* **1934**, *88*, 83.
- (37) Redlich, O.; Nielsen, L. E. *J. Am. Chem. Soc.* **1943**, *65*, 654.
- (38) Redlich, O.; Bigeleisen, J. *J. Am. Chem. Soc.* **1943**, *65*, 1883.
- (39) Krawetz, A. A. PhD Thesis; University of Chicago, Chicago, IL, 1955.
- (40) Minogue, N.; Riordan, E.; Sodeau, J. R. *J. Phys. Chem. A* **2003**, *107*, 4436.
- (41) Martin, E.; George, C.; Mirabel, P. *Geophys. Res. Lett.* **2000**, *27*, 197.